Journal of Atmospheric and Solar–Terrestrial Physics 190 (2019) 96–107

Contents lists available at ScienceDirect

Journal of Atmospheric and Solar-Terrestrial Physics

journal homepage: www.elsevier.com/locate/jastp

On the seasonal and solar cycle variation of the ULF fluctuations at low latitudes: A comparison with the ionospheric parameters

U. Villante [a,b,*], P. Tiberi [a,b], M. Pezzopane [c]

[a] Dipartimento di Scienze Fisiche e Chimiche, Università, L'Aquila, Italy
[b] Consorzio Area di Ricerca in Astrogeofisica, L'Aquila, Italy
[c] Istituto Nazionale di Geofisica e Vulcanologia, Via di Vigna Murata 605, 00143, Roma, Italy

ARTICLE INFO

Keywords:
ULF waves
Seasonal variation
Solar cycle variation
Dawn terminator

ABSTRACT

A long term analysis (1996–2015) of the occurrence and characteristics of the wave events (Pc3; $f = 20$–100 mHz; H and D component), detected at a low latitude ground-based station (L'Aquila, Italy), and the comparison with the ionospheric parameters reveal some interesting aspects of their seasonal and solar cycle variation. In general, the daytime wave activity, which basically consists of penetrating upstream waves and, at higher frequencies, of resonances of local field lines, appears more intense (with a more relevant percentage of D events) in winter than in summer, suggesting a seasonal dependence of the attenuation and rotation of the downgoing signal through the ionosphere and, during winter, less efficient ionospheric conditions for the onset of resonance processes (typically occurring along the H component). This situation persists during solar minima, while, during solar maxima, the summer occurrence rate of events exceeds the winter one: this aspect might be related to the more frequent impact on the magnetosphere of energetic solar wind structures during solar maxima; in summer, given the favourable ionospheric conditions, they might determine a much more frequent manifestation of relevant resonance events. Rapidly increasing after midnight, the wave activity reveals a pre-sunrise peak followed by a minimum, on average coincident with the *fo*F2 minimum, and the winter pattern appears to be delayed ≈1 h compared to the summer one.

1. Introduction

Long term analysis of the occurrence and characteristics of relevant wave events in the mid-frequency ULF range ($f \approx 10$–100 mHz; reviews by Villante, 2007; Menk, 2013), conducted at a low latitude ground-based station (L'Aquila, AQU, Italy, geomagnetic coordinates $\lambda \approx 36.1°$ N, $\varphi \approx 87.0°$ E; $L \approx 1.6$; LT = UT+1; Villante and Tiberi, 2015; Villante and Tiberi, 2016), evidenced that these fluctuations mostly occur between dawn and noon, in the Pc3 band ($f \approx 22$–100 mHz); they typically manifest, as almost regular, long-living waveforms, propagating antisunward, ultimately related to upstream waves generated in foreshock region. Several channels for the propagation to the ground of these fluctuations have been proposed (review by Olson and Fraser, 1994): direct propagation of compressional waves through the magnetosheath and the magnetosphere; penetration at the cusp; coupling to an evanescent mode at the plasmapause, and others. Transported across the dayside magnetosphere as fast magnetosonic modes, the waves partially convert their energy into standing Alfvèn waves, where the frequency of the incoming wave matches the frequency of the local field line; consequently, the wave modes manifest also as resonances of local field lines (FLRs; standing waves on field lines with fixed ends on conjugate hemispherical points). In the magnetosphere, the upstream waves are mostly compressional and the FLRs mostly toroidal. The wave characteristics modify across the ionosphere: the fast modes do not experience any absorption at nightside and are weakly absorbed at dayside; the absorption of the Alfvèn waves is expected to be low at dayside, significantly increasing at nightside (Pilipenko et al., 2008). In addition, a ≈90° rotation of the polarization ellipse across the ionosphere is expected only for the toroidal component; so, both the upstream waves and the FLRs would show up mostly along the H component (north--south) on the ground. On the other hand, the coupling between modes may result in an Alfvèn wave with a poloidal component and the actual amount of rotation of the polarization ellipses may differ from the predicted one (Heilig et al., 2013); in addition, since the signals detected at ground-based stations are integrated over a large area of the ionosphere, they might have mixed contributions from the Alfvèn wave and from the

* Corresponding author. Dipartimento Scienze Fisiche e Chimiche, Università, L'Aquila, 67100, Italy.
E-mail address: umberto.villante@aquila.infn.it (U. Villante).

https://doi.org/10.1016/j.jastp.2019.05.005
Received 3 February 2019; Received in revised form 2 April 2019; Accepted 7 May 2019
Available online 10 May 2019
1364-6826/© 2019 Elsevier Ltd. All rights reserved.

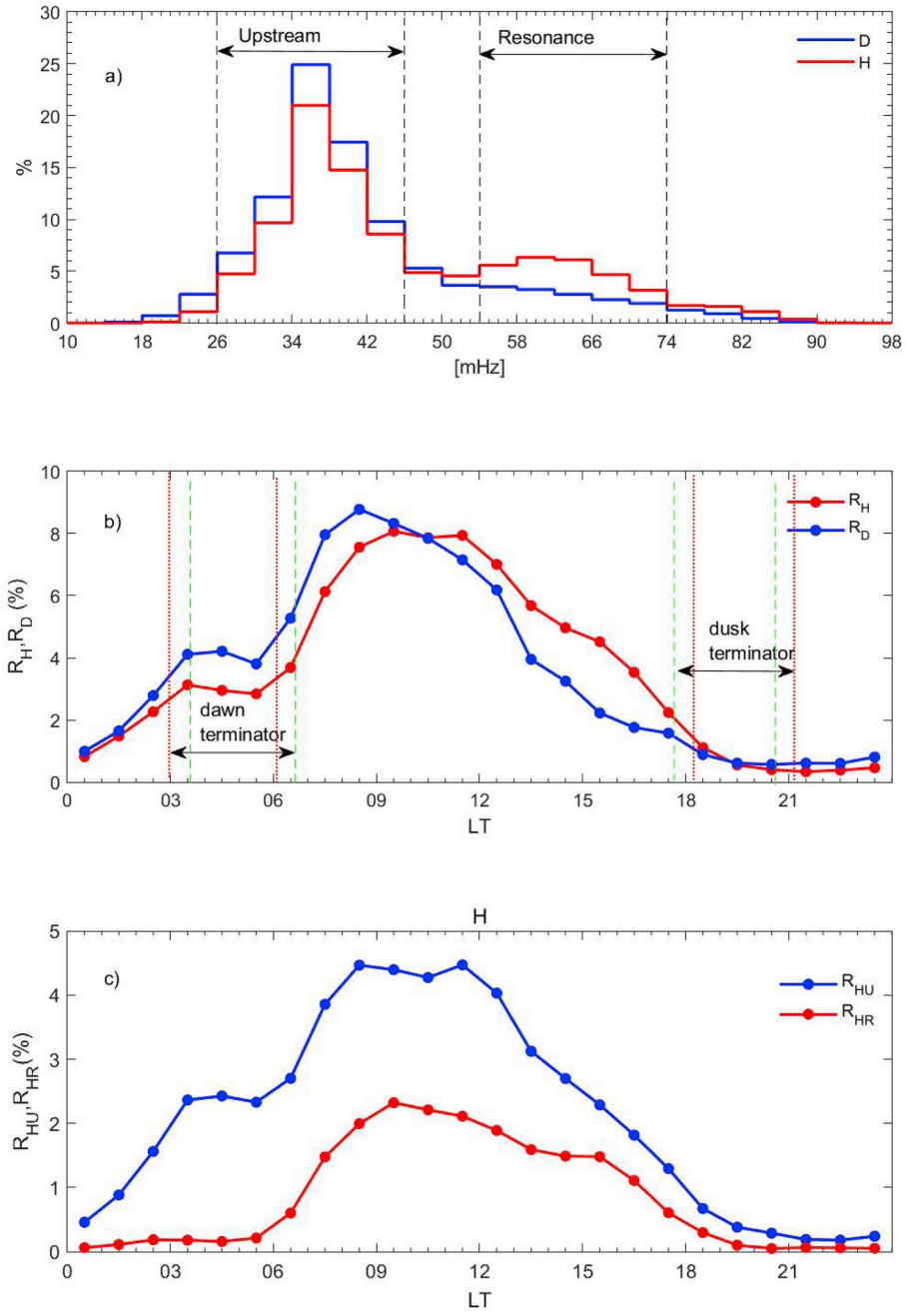

Fig. 1. a) The frequency distribution of the selected events (D component, blue; H component, red). b) The hourly rate of occurrence of D (blue) and H events (red). The dashed green lines delimit the estimated LT ranges of the dawn and dusk terminators at 100 km of altitude during the year; the dotted red lines delimit those of the terminator at 250 km of altitude. c) The hourly rate of occurrence of H events in the upstream band (blue) and in the resonance band (red). (For interpretation of the references to colour in this figure legend, the reader is referred to the Web version of this article.)

fast mode: as a matter of fact, clear evidence for ULF waves is routinely detected in ground-based measurements also along the D component (east/west). Much less frequent, impulsive, damped oscillations, ultimately related to the substorms onset, occur during the night (Pi2; $f \approx 6$–25 mHz; Keiling and Takahashi, 2011).

Some aspects of the analysis conducted by Villante and Tiberi (2015) and Villante and Tiberi (2016) suggested long term and seasonal modulations of the wave occurrence and characteristics: these features are more deeply analysed in the present paper in which the aspects of the wave manifestation are compared with measurements performed at the ionospheric station of Rome ($\lambda \approx 42.0^\circ$ N, $\varphi \approx 93.8^\circ$ E) by means of an AIS-INGV ionosonde (Zuccheretti et al., 2003) and validated by using the Interpre software (Pezzopane, 2004).

2. The event identification

For the scopes of the present investigation, we examined almost twenty years of data (March 1996–December 2015) collected at AQU, encompassing the solar cycle 23 (1996–2008) and a major portion of the solar cycle 24, with several data gaps (the largest occurring between January–June 2012 and between October 2014–February 2015): in the period of interest, the solar maxima occurred approximately at November 2001 and April 2014, respectively; a prolonged deep minimum, during ≈2008–2009, was characterized by a decrease of ≈15% in the EUV solar radiation with respect to the previous one (Chen et al., 2011, 2012; Perna and Pezzopane, 2016).

The details of the data analysis, power spectra evaluation and event identification have been extensively discussed by Villante and Tiberi (2015): here, we simply remind that, during less active periods (i. e. $Kp<5$, $Dst>-100$), the dominant peak is identified, in the 5 min spectra

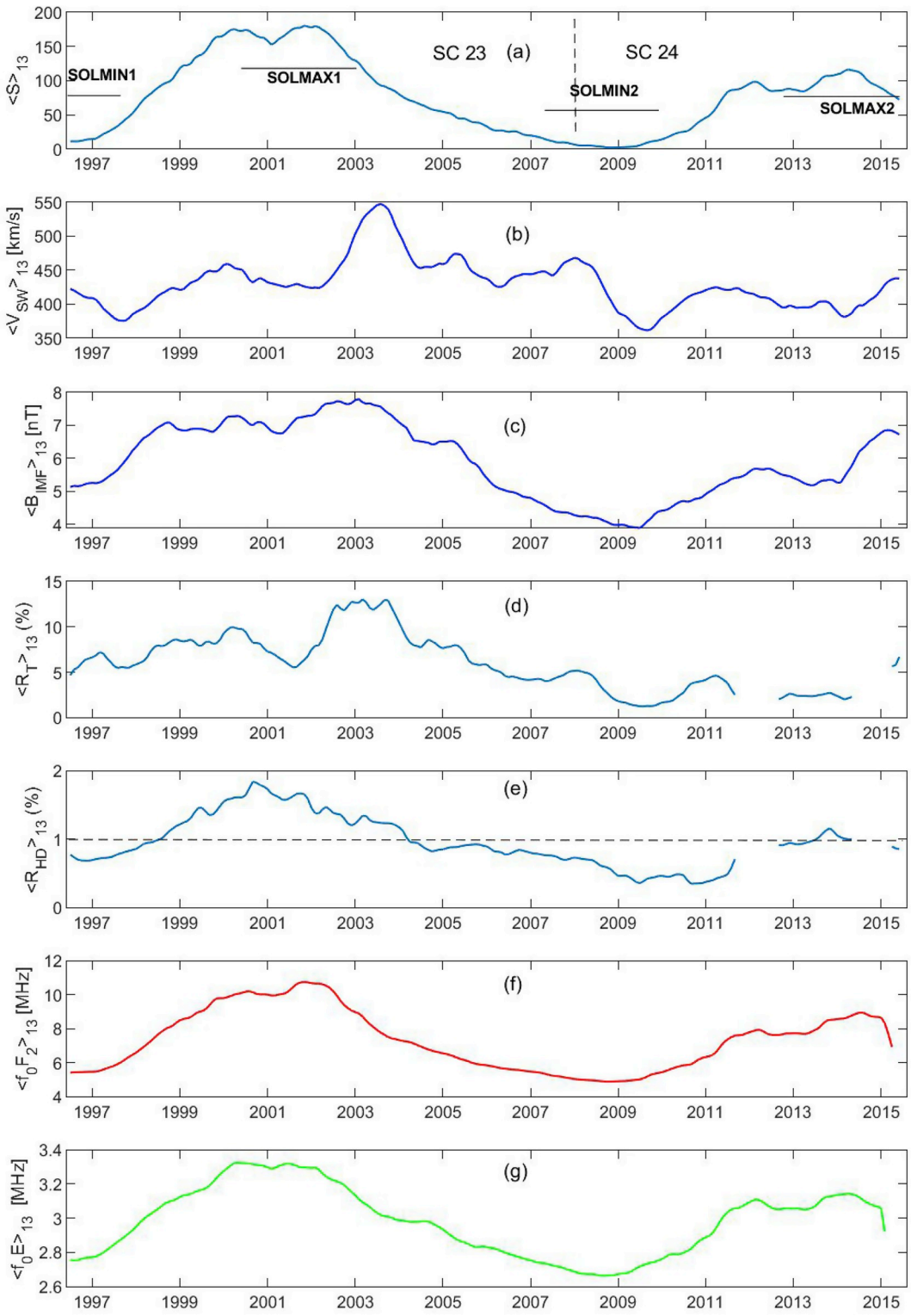

Fig. 2. The 13-months running averages of several parameters. From the top: the sunspots number ($<S>_{13}$, panel a), the solar wind speed ($<V_{SW}>_{13}$, panel b), the interplanetary magnetic field strength ($<B_{IMF}>_{13}$, panel c), the total occurrence rate of events ($<R_T>_{13}$, panel d), the relative occurrence ($<R_{HD}>_{13}$, panel e); the 13-months medians of the daytime values of the ionospheric parameters ($<foF2>_{13}$, panel f) and ($<foE>_{13}$, panel g).

of the H and D component, with a spectral resolution of 4 mHz in the frequency range $f = 10$–100 mHz; this peak is then selected as relevant "event" if the signal to noise ratio exceeds a given threshold T (different for H and D, given the greater amplitude of H events). In practise, we selected a large number of events over the entire period (namely, $N_D = 50{,}888$ and $N_H = 50{,}841$; with H events more energetic). Obviously, the event identification is influenced by the magnetospheric conditions in that sharp, narrow band peaks more rarely emerge in the power spectra during more active periods. In the following, we consider the hourly occurrence rates, R_H and R_D (the ratios between the number of events and the number of available 5 min intervals in each hour), their ratio $R_{HD} = R_H/R_D$ and the total occurrence rate $R_T = R_H + R_D$ (counting

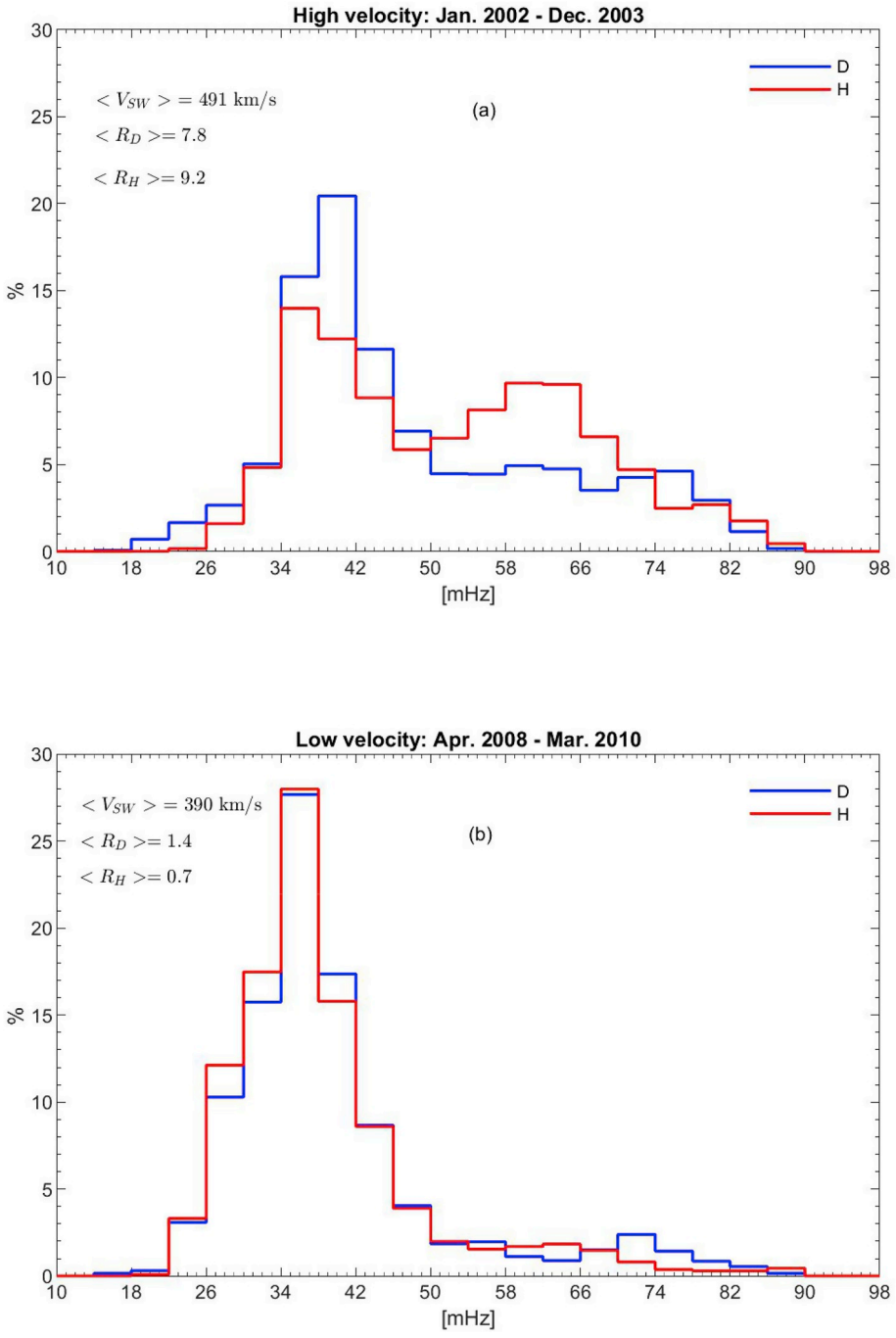

Fig. 3. a) The frequency distribution of the selected events (D component, blue; H component, red) during high solar wind velocity intervals. b) The frequency distribution of the selected events during low solar wind velocity intervals. $<W_{SW}>$, $<R_D>$ and $<R_H>$ are the average SW velocity and occurrence rates during high and low velocity intervals, respectively. (For interpretation of the references to colour in this figure legend, the reader is referred to the Web version of this article.)

once the events simultaneously identified in both components); the ionospheric conditions are represented by the hourly validated values of the F2-layer and E-layer critical frequencies, namely *fo*F2 and *fo*E, both related to the corresponding electron densities through the well-known relationship $fo=(N/(1.24\cdot10^4))^{1/2}$, where *fo* is the frequency in MHz and *N* the electron density in el/cm^3. Ionospheric data were downloaded from the electronic Space Weather upper atmosphere database of INGV (http://www.eswua.ingv.it/; Romano et al., 2008).

3. The characteristics of the ULF activity

The occurrence and characteristics (practically the same discussed by Villante and Tiberi, 2015 and Villante and Tiberi, 2016) of the events selected over the entire period are summarized in Fig. 1. Briefly, a major fraction of the events have frequencies between $f\approx$ 26–46 mHz ("upstream band"; Fig. 1a) and basically consist of penetrating upstream waves influencing both components; at higher frequencies, the percentages of the H events exceed the D ones, particularly between $f\approx$ 54–74 mHz ("resonance band") and reflect the occurrence of FLRs, mostly influencing the H component: at our station, indeed, during the preceding solar cycle (1985–1994; Vellante et al., 1996), the resonance frequency was found to vary approximately between $f\approx$ 60–90 mHz, with lower frequencies at solar maximum. Actually, the FLRs influence, at some extent, also the D component (Heilig et al., 2013); however, the

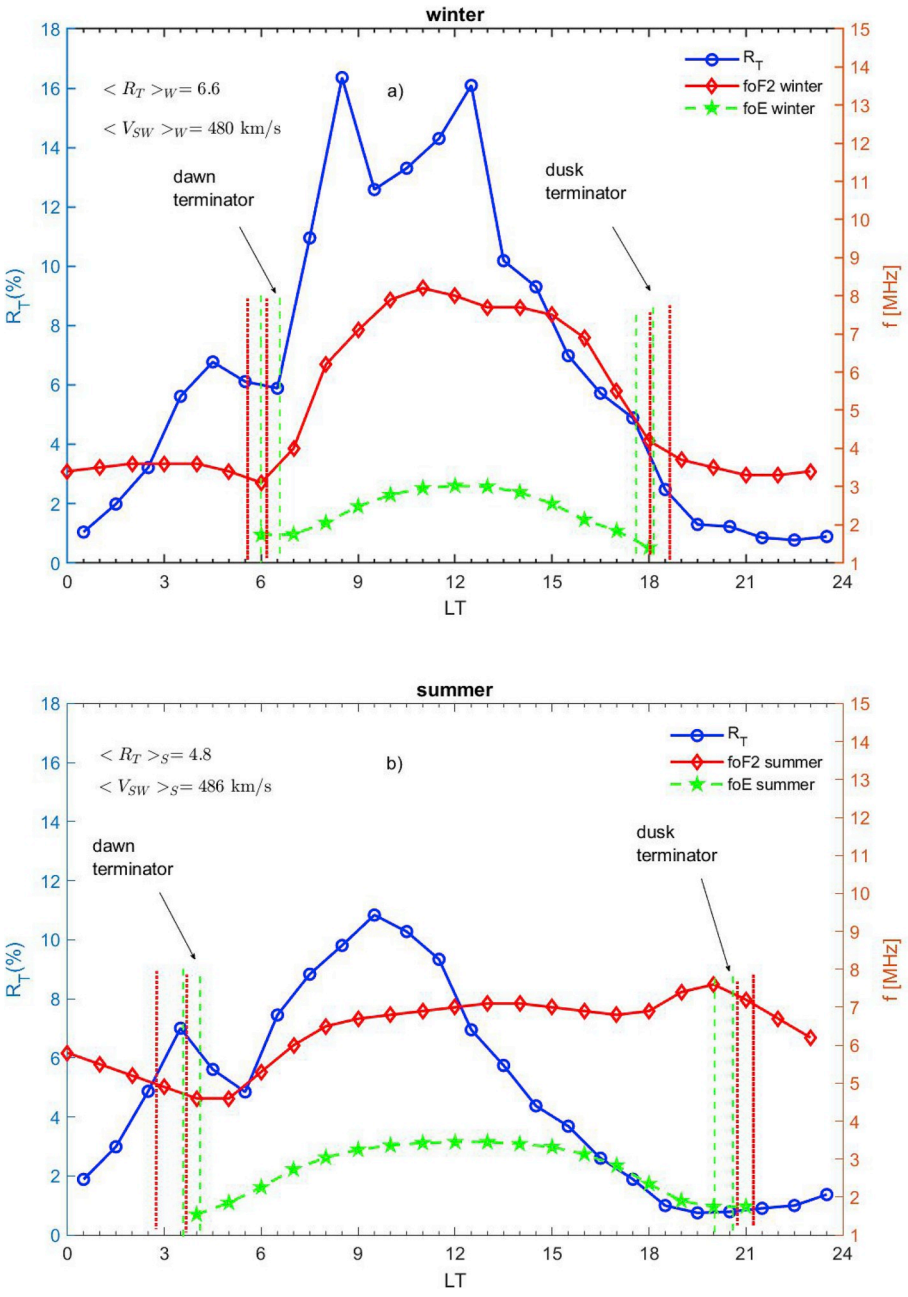

Fig. 4. a) The hourly rate of occurrence of events (blue trace); the hourly values of the F2- and E-layer critical frequencies (*fo*F2, red; *fo*E, green). The dashed green lines delimit the estimated LT ranges of the dawn and dusk terminator at 100 km of altitude during winter; the dotted red lines delimit those of the terminator at 250 km of altitude. b) The same as a) during summer. (For interpretation of the references to colour in this figure legend, the reader is referred to the Web version of this article.)

corresponding enhancements rarely emerge as dominant peaks in the power spectra. As a matter of fact, while the selected D events are mostly related to the upstream waves, the H events are a mixture of upstream waves (in general, much more numerous) and FLRs. The LT dependence of the occurrence rates (Fig. 1b) confirms the ULF activity mostly as a dayside phenomenon, with highest rates between ≈08 and 10 LT (R_D) and between ≈09 and 12 LT (R_H); the wave activity declines in the afternoon and rarely occurs in the pre-midnight sector (≈21–24 LT). The average rates are quite relevant between ≈04 and 07 LT, a sector practically delimited by the LT excursion of the dawn terminator during the year (the dashed green lines in Fig. 1b delimit the estimated LT ranges of the dawn and dusk terminator at 100 km, in the highly conducting E layer, ≈03:40–06:38 LT, ≈17:34–20:32 LT, respectively; the dotted red lines delimit those of the terminators at 250 km, in the F layer, ≈02:57–06:05 LT, ≈18:07–21:16 LT): as a matter of fact, rapidly increasing after midnight, both R_D and R_H reach a plateau between ≈03 and 05 LT; then, they slightly decrease at ≈05–06 LT, more explicitly in R_D; by contrast, no peculiar feature emerges in the region of the dusk terminator. Note also that, in general, the selected D events are predominant with respect to H events between ≈03 and 09 LT while the opposite situation occurs in the afternoon. On average, the ratio between the after-sunrise and the pre-sunrise rates is ≈ 2; according to Yagova et al. (1999), who examined a 5 days period characterized by a rather high ULF wave activity, the ratio of the after-sunrise intensity to the pre-sunrise intensity would be ≈ 1.6 at $L \approx 1.6$; Tanaka et al. (2007) found that the amplitude of Pc3 fluctuations detected between $L \approx 1.0$–2.1 is ≈ 2–4 times greater after dawn than before dawn and is greater at higher latitudes. Fig. 1c compares, for the H-component, the LT variation of the occurrence rates in the upstream (R_{HU}, blue trace) and in the resonance band (R_{HR}, red trace). It clearly shows that, while the higher frequency activity is confined within the daytime sector, before ≈06 LT the wave activity is due only to the lower frequency events: their morphology, waveforms and duration reveal that they mostly consist of penetrating upstream waves, with an additional

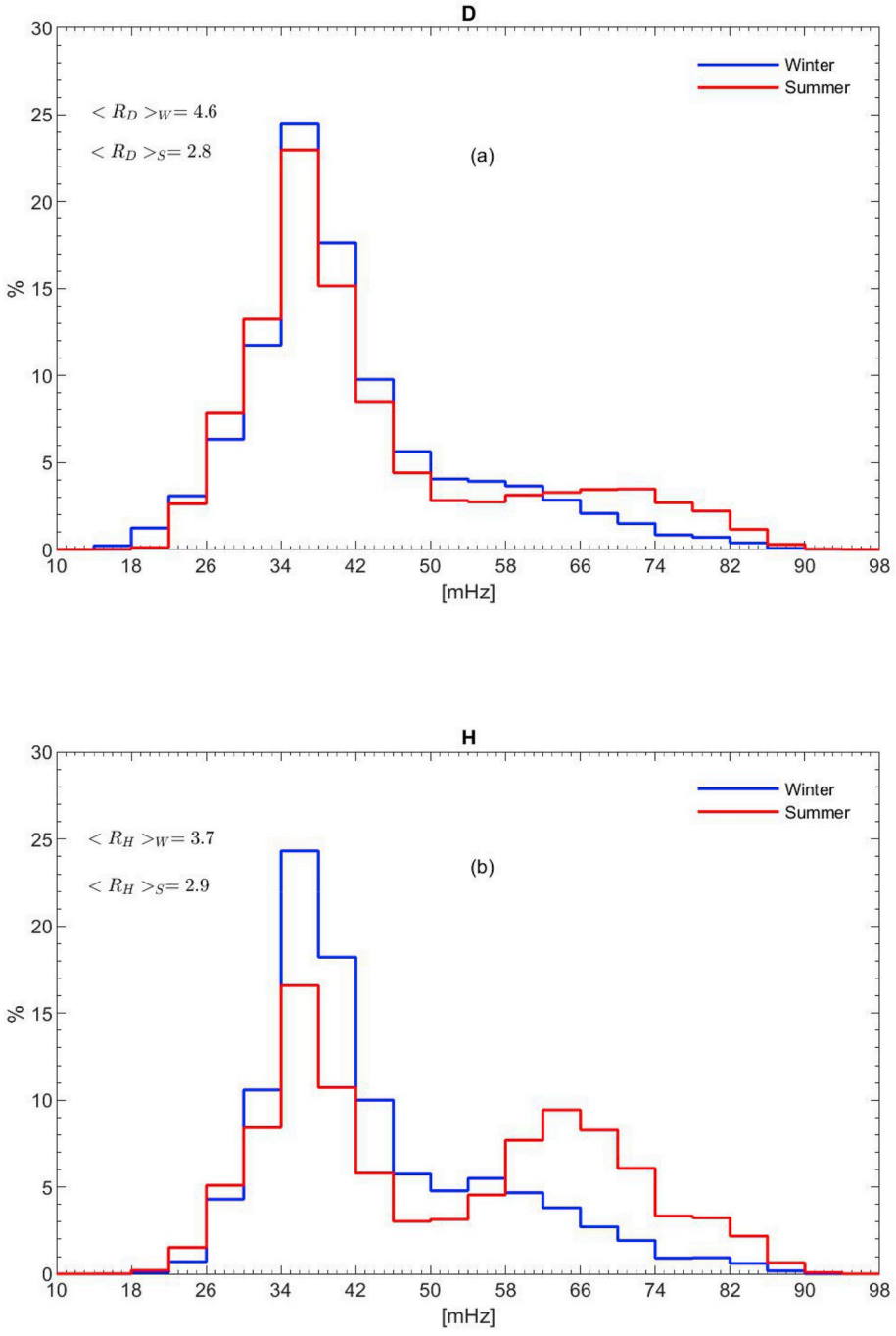

Fig. 5. a) The frequency distribution of selected D events (panel a; blue for winter, red for summer); H events (panel b). (For interpretation of the references to colour in this figure legend, the reader is referred to the Web version of this article.)

contribution of Pi2 waves, more relevant around midnight (Villante and Tiberi, 2016). In general, in the scientific literature, the occurrence of ULF waves in the dark hemisphere has been mostly attributed to waves locally excited in association with substorms; nevertheless, in agreement with the present results, several papers presented evidence for upstream waves in the night sector: namely, Takahashi et al. (2005) discussed a nighttime Pc4 event ($f \approx 5$–20 mHz) originating upstream of the bow shock and detected at low latitudes ($L < 2$); Ponomarenko et al. (2010) reported magnetometer and radar observations in support of the propagation of upstream waves to the nightside; Takahashi et al. (2016) presented evidence for ULF waves of upstream origin propagating to the midnight sector of the inner magnetosphere; lastly, Yagova et al. (2017), from one year of Pc3 observations between $L \approx 1.45$–1.83, found two groups of nighttime Pc3 fluctuations: the counterpart of morning Pc3 and the locally generated Pc3, probably associated with non-substorm bursty processes.

4. The long term variation and the role of the SW speed

Fig. 2 shows the 13-months running averages of several parameters (evaluated when at least 75% of the expected data are available): the sunspots number ($<S>_{13}$); the solar wind speed ($<V_{SW}>_{13}$); the interplanetary magnetic field strength ($<B_{IMF}>_{13}$); the total occurrence rate of events ($<R_T>_{13}$); the relative occurrence ($<R_{HD}>_{13}$; in addition, it shows the 13-months medians of the daytime values of the *fo*F2 and *fo*E parameters. As evidenced by the *S* behavior, the solar cycle 23 is more

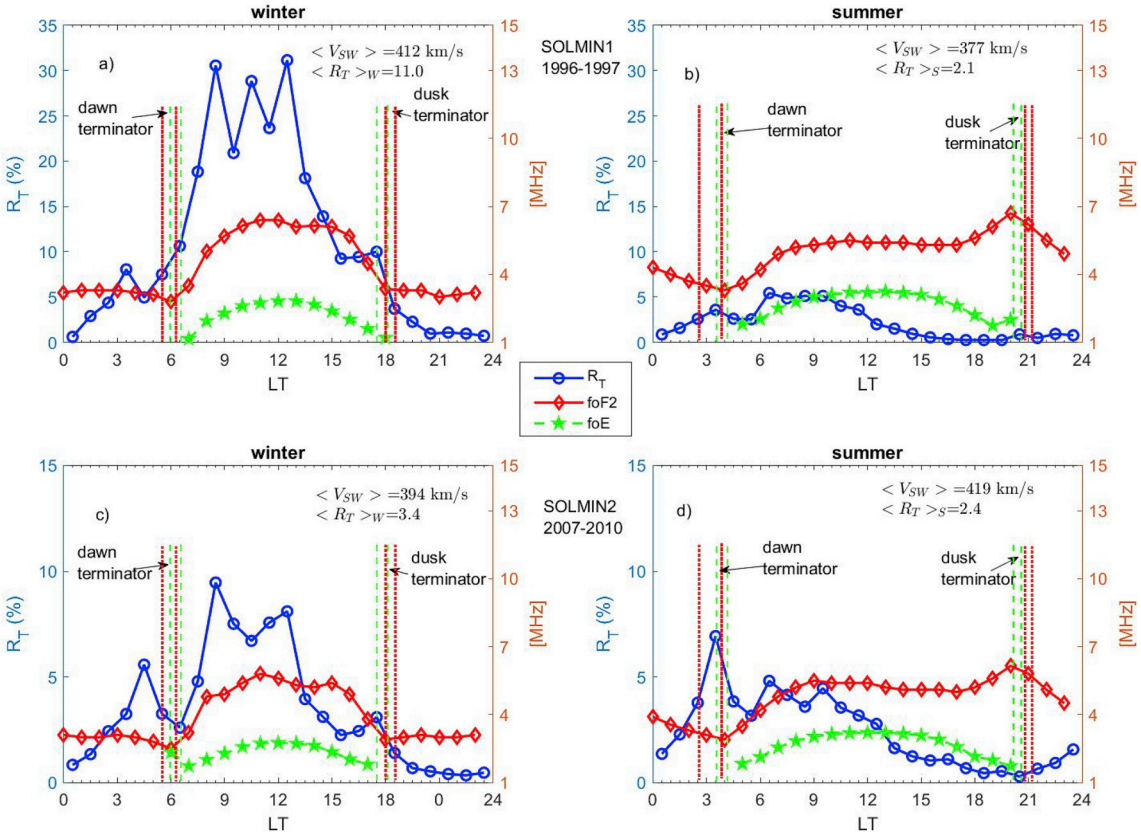

Fig. 6. a) The hourly rate of occurrence of events (blue trace); the hourly values of *fo*F2 (red) and *fo*E (green) during winter for SOLMIN1. The dashed green lines delimit the estimated LT ranges of the dawn and dusk terminator at 100 km of altitude; the dotted red lines delimit those of the terminator at 250 km of altitude. b) The same as a) during summer. c) The hourly rate of occurrence of events (blue trace); the hourly values of *fo*F2 (red) and *fo*E(green) during winter for SOLMIN2. d) The same as c) during summer. (For interpretation of the references to colour in this figure legend, the reader is referred to the Web version of this article.)

active than the solar cycle 24; the SW speed is high during ≈2003 (with peak values such as $<V_{SW}>_{13}$≈550 km/s, centered on August) and low during ≈1997 ($<V_{SW}>_{13}$≈375 km/s; September) and during ≈2009 ($<V_{SW}>_{13}$≈360 km/s; August); the average IMF during ≈1999–2003 ranged between ≈6.5–7.5 nT (with highest values between ≈ Sept. 2002–March 2003) while attained minimum values of ≈4–4.5 nT during ≈2007–2009 (with lowest intensities between ≈ October 2008–May 2009): according to the well-known relationship between the frequency of the upstream waves, f_u, and B_{IMF} (f_u (mHz) ≈k*B_{IMF} (nT); $k \approx 6$, according to Troitskaya et al., 1971; Troitskaya, 1994) and consistent with Fig. 1a, the upstream waves, over the entire period, would be mostly expected between $f \approx$ 28–42 mHz. The trends of $<foF2>_{13}$ and $<foE>_{13}$ basically reflect the long term modulation of the sunspot number (Davies, 1990; Hargreaves, 1995). The occurrence rate of events, $<R_T>_{13}$, is, in general, much higher during solar cycle 23 than during the deep solar minimum and the rising phase of solar cycle 24. Clearly influenced by V_{SW} (Yedidia et al., 1991; Villante and Tiberi, 2015), $<R_T>_{13}$ attains highest values during ≈2002–2003. The $<R_{HD}>_{13}$ behavior shows that the selected H events (more energetic) are relatively more frequent during higher solar activity conditions while, during the deep minimum, the D events are, on average, almost twice as frequent as the H events.

Separate analysis of the wave characteristics for periods of high and slow V_{SW} confirm (Yedidia et al., 1991) that during high V_{SW} (Fig. 3a, 2002–2003), when the upstream waves reveal, in the D component, higher percentages at $f \approx$ 34–46 mHz (consistently, the average IMF, in the period of interest, would suggest a favorite range $f_u \approx$ 38–46 mHz), the FLRs are strongly favored and reveal higher percentages between $f \approx$ 58–66 mHz; almost as frequent as the upstream waves in the H distribution, the FLRs manifest, at some extent, also in the D distribution. By contrast, during low V_{SW} (Figs. 3b and 2008–2010), the frequency distributions of the D and H events (very similar) reveal more pronounced percentages at $f \approx$ 30–42 mHz ($f_u \approx$ 26–34 mHz for $k \approx 6$; in this time interval the results are better consistent with the value $k \approx 7$ proposed by Ponomarenko et al., 2002). In this case the FLRs are extremely rare, an aspect consistent with the results obtained by Vellante et al. (2007) who concluded that, at our latitude, the FLRs are rare during quiet magnetospheric conditions (<10% for $Kp < 1$). Interestingly, in this case, due to the extremely low rates of H events, some signatures of FLRs are better identified, above $f \approx$ 70 mHz, in the D component.

5. The seasonal dependence

In order to examine the seasonal dependence of the ULF occurrence and characteristics we compared in Fig. 4 the results obtained during the winter solstice season (November, December, January, for the entire period 1996–2015) with those obtained during the summer solstice season (May, June, July, for the entire period 1996–2015; different choices of the time intervals do not affect significantly our results).

As usually observed, in winter, the daytime level of *fo*E is lower (on average, ≈2.7 MHz; Fig. 4a) and less extended in time (≈06–18 LT) than in summer (≈3.3 MHz; ≈04–21 LT; Fig. 4b); on the contrary, consistent with the so called "winter anomaly" (i. e., the daytime electron densities in the F2 layer are larger in winter than in summer; Rishbeth and Garriot, 1969; Rishbeth et al., 2000; Ezquer et al., 2014; Perna et al., 2017), the daytime average level of *fo*F2 in winter (≈7.5 MHz) is higher than in summer (≈6.9 MHz; see Pietrella et al., 2012, for a long term analysis of the *fo*F2 variability over Rome). Remarkably, the results obtained for the event occurrence reveal that, practically for the same average SW speed ($<V_{SW}>_w \approx$ 480 km/s; $<V_{SW}>_s \approx$ 486 km/s; subscripts "w" and "s"

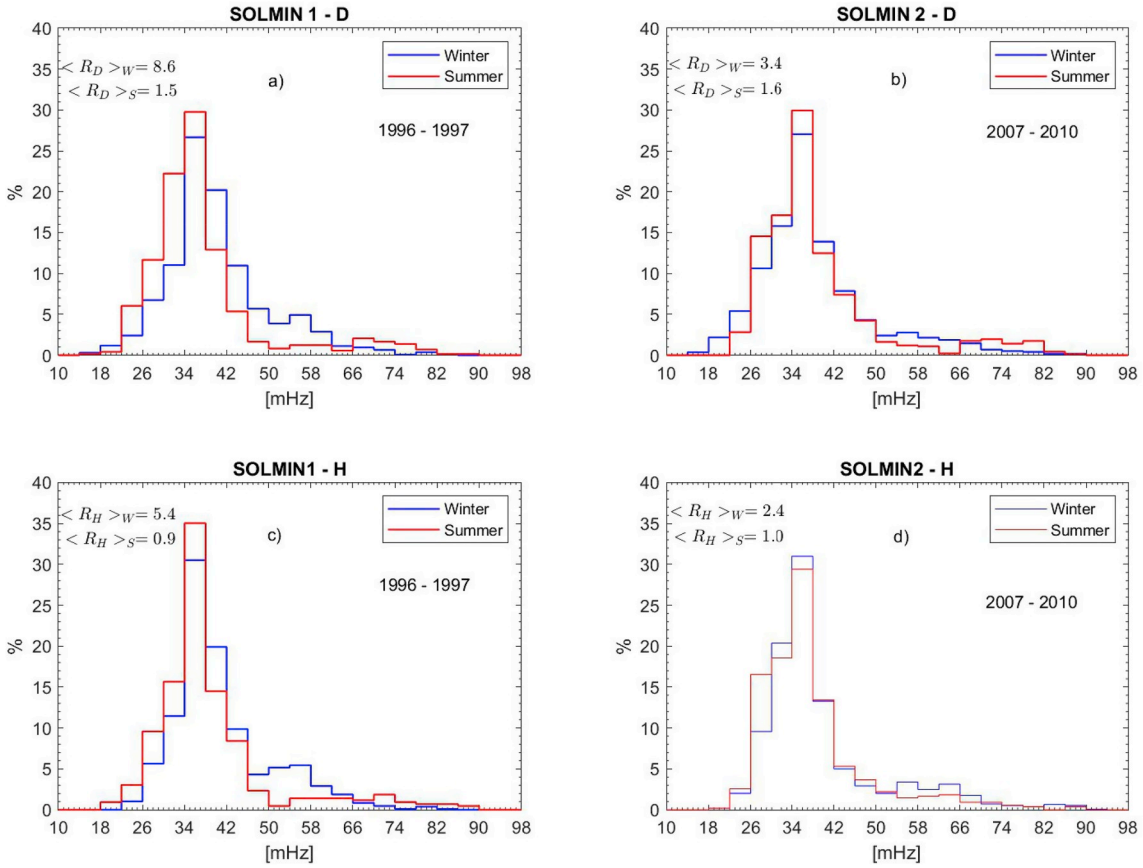

Fig. 7. a) The frequency distribution of the selected D events (winter, blue trace; summer, red trace) for SOLMIN1. b) The frequency distribution of the selected D events for SOLMIN2. c) The frequency distribution of the selected H events for SOLMIN1. d) The frequency distribution of the selected H events for SOLMIN2. (For interpretation of the references to colour in this figure legend, the reader is referred to the Web version of this article.)

stand for winter and summer respectively), the wave activity is, in general, ≈40% more intense in winter ($<R_T>_w \approx 6.6$, $<R_T>_s \approx 4.8$) and ≈60% in the daytime ($<R_T>_w \approx 13.2$, $<R_T>_s \approx 8.1$).

The comparison of the LT dependencies shows several interesting aspects. Indeed, in winter, both *fo*F2 and R_T sharply increase after ≈07 LT, while in summer, smoother increases of these parameters occur after ≈06 LT. In winter, R_T shows two prominent peaks of comparable height at ≈08–09 LT (morning peak) and at ≈12–13 LT (noon peak); in summer, a broad and less pronounced R_T enhancement occurs between ≈08 and 12 LT (peaked at ≈09–10 LT). In the afternoon, the wave activity rapidly decreases in both seasons while the *fo*F2 level persists high in summer. In the pre-morning sector, R_T shows, in winter, a peak at≈04–05 LT and a minimum at ≈06–07 LT; in summer, the R_T profile is more pronounced, with a prominent peak at ≈03–04 LT, followed by a minimum, approximately 2 h later (≈05–06 LT); interestingly, in both seasons, the R_T and *fo*F2 minima are almost simultaneous. In practise, in the pre-morning sector, the winter pattern appears to be delayed ≈1 h compared to the summer one: this feature determines the observed plateau of R_T between ≈05 and 07 LT, when the wave occurrence is averaged over a whole year (Fig. 1b; interestingly, a similar plateau in the global wave activity appears between ≈06:30–07:30 LT in earliest analysis of the ULF occurrence at $\lambda \approx 49°$; see Fig. 5 of Saito,1964). On the contrary (although rarely remarked), a drop in the wave intensity, preceding the morning increase, appears in several figures related to short term analysis (for example, Fig. 5 in Yagova et al., 1999). On average, the ratio between the morning and the pre-sunrise peak is ≈ 2.4 in winter and ≈1.5 in summer.

The comparison of the frequency distributions (Fig. 5) shows, during the winter, a reduced FLRs occurrence and the wave activity, on both components (blue traces in both panels), is mostly due to the penetrating upstream waves; during the summer (red traces), the FLRs provide, at higher frequencies, a relevant contribution on the distribution of the H events (much poorer in the D distribution); remarkably, although less frequent, the winter FLRs, on average, show lower frequencies than the summer ones.

6. The solar cycle dependence

To analyse the aspects related to the solar cycle variation, we focused on the solar minima and maxima considering the following intervals: SOLMIN1: May 1996–July 1997; SOLMAX1: May 2000–January 2003; SOLMIN2: May 2007–January 2010; SOLMAX2: November 2012–July 2015 (see Fig. 2a); except for SOLMIN1 (including one winter solstice and two summer solstices), each interval includes three winter and three summer solstices. As recently detailed by Burns et al. (2014), who conducted a long term analysis (2000–2011) at stations located between $\lambda \approx +/-50°$, it is useful to remind that the winter anomaly is significant at solar maximum and virtually not existent at solar minimum. As we show in the following, in substantial agreement, in our case, during solar minima, the winter and the summer *fo*F2 average levels are more or less comparable while during solar maxima the winter levels largely exceed the summer ones.

6.1. Solar minima

During SOLMIN1, the winter level of *fo*F2 between 09 and 15 LT (≈6.0 MHz; Fig. 6a) exceeds by ≈ 10% the summer one (≈5.4 MHz; Fig. 6b); in this case, for slightly greater SW speeds, the winter rate of events ($<R_T>_w \approx 11.0$) far exceeds the summer one ($<R_T>_s \approx 2.1$), with an average ratio such as ≈5.2. During the winter, moreover, a peak

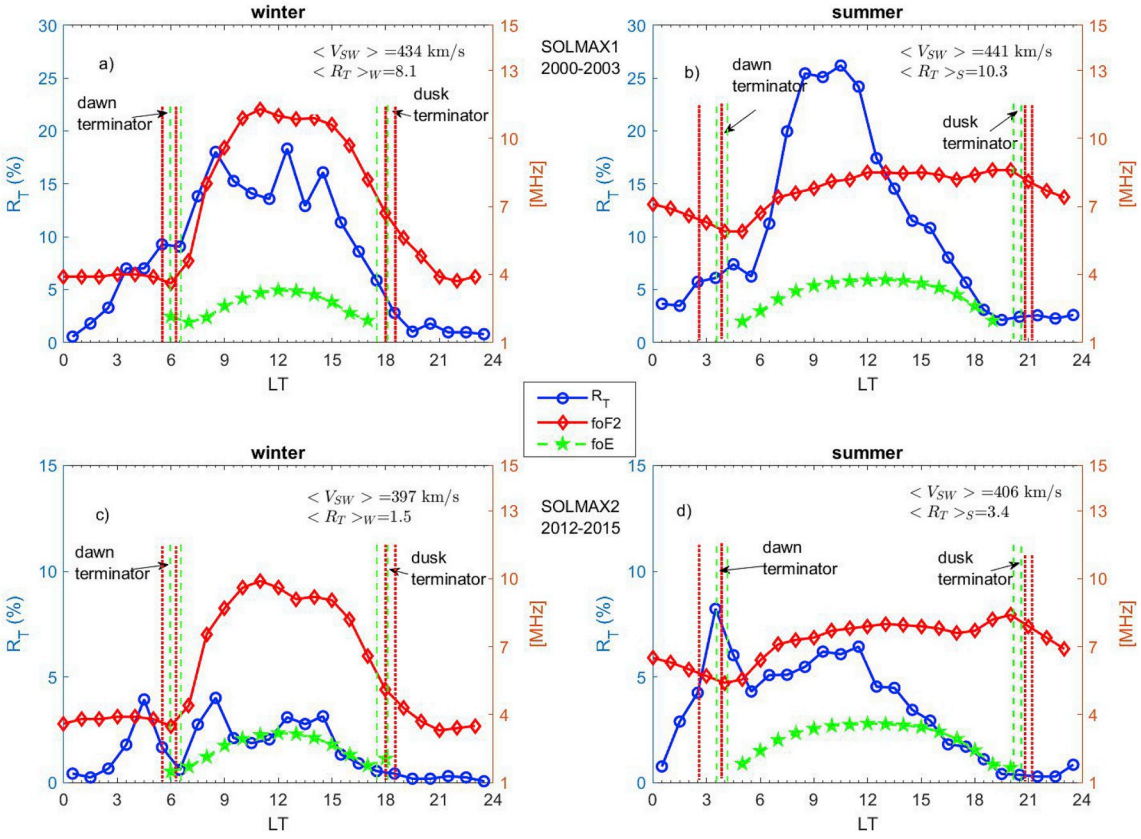

Fig. 8. a) The hourly rate of occurrence of events (blue trace); the hourly values of *fo*F2(red) and *fo*E (green) during winter for SOLMAX1. The dashed green lines delimit the estimated LT ranges of the dawn and dusk terminator at 100 km of altitude; the dotted red lines delimit those of the terminator at 250 km of altitude. b) The same as a) during summer. c) The hourly rate of occurrence of events (blue trace); the hourly values of *fo*F2 (red) and *fo*E (green) during winter for SOLMAX2. d) The same as c) during summer. (For interpretation of the references to colour in this figure legend, the reader is referred to the Web version of this article.)

emerges at ≈03–04 LT, the early morning variation is steep, the dayside activity is intense (with three peaks at ≈09 LT, ≈11 LT, ≈13 LT); in addition, some evidence for a R_T enhancement occurs near the dusk terminator (≈16–18 LT), when *fo*F2 rapidly decreases. During the summer (Fig. 6b), small R_T enhancements occur at ≈03–04 LT and at ≈06–07 LT and the daytime wave activity is depressed. A similar situation occurs during SOLMIN2: in this case, the winter (Fig. 6c) and the summer level of *fo*F2 (Fig. 6d) are practically the same in the dayside (≈5.3 MHz) and, despite a SW speed somewhat lower than in summer, the ratio between the winter and the summer event occurrence is ≈ 1.4 for the entire day and ≈2.2 between 09 and 15 LT. During the winter, a prominent peak occurs at ≈04–05 LT and the associated minimum is simultaneous to the *fo*F2 one (≈06–07 LT); as for the previous case, in addition to the morning and noon peak, an R_T enhancement occurs near the dusk terminator (accompanied by a *fo*F2 decrease). Noticeably, during the summer, the R_T peak at ≈03–04 LT sharply exceeds the daytime rates. The results in Fig. 7 show that, during both minima, the highest percentages of upstream waves occurred between f = 30–38 mHz (i. e., practically the same range found by Vellante et al., 1996; f = 30–40 mHz during 1985). On the other hand, contrary to Vellante et al. (1996), who found FLRs above f = 80–85 mHz during solar minima, the summer distributions of H events do not show any clear evidence for relevant FLRs contributions: likely, this aspect might be related to the poor occurrence of H events (<R_T> ≈1%) due to the low SW speed characterizing SOLMIN1 (<V_{SW}>≈375 km/s) and to the extremely quiet magnetospheric conditions and reduced EUV radiation characterizing SOLMIN2.

6.2. Solar maxima

During SOLMAX1, the SW speeds in winter (Fig. 8a) and in summer (Fig. 8b) are comparable while the daytime winter level of *fo*F2 (≈10.4 MHz) exceeds the summer level (≈8.2 MHz); in this case, differently from solar minima, the global summer occurrence exceeds the winter one with a ratio ≈1.3, an aspect more pronounced in the morning sector. In both seasons the pre-dawn R_T peaks are less explicit than in other cases; during the winter, R_T confirms the morning and the noon peaks; during the summer, the broad R_T enhancement occur at ≈10–12 LT. During SOLMAX2 (much less active; Fig. 8c), the winter *fo*F2 level (≈9.1 MHz) exceeds the summer level in the dayside (≈7.7 MHz); the summer occurrence rate (for comparable SW speeds) exceeds the winter one, on average by a factor ≈2.2. During the winter, the R_T peaks occurring at ≈04–05 LT and at ≈08–09 LT are comparable. As for SOLMIN2, in this solar cycle, during the summer, a dominant peak emerges at ≈03–04 LT, well above the daytime level. The frequency distributions (Fig. 9) shows that, at both solar maxima, the upstream waves mostly ranges between f = 34–46 mHz, suggesting a solar cycle modulation of the frequency of the upstream waves smaller than that one found by Vellante et al. (1996; f ≈ 50 mHz during 1989–1991); note also that during periods of higher solar activity (SOLMAX1), the higher summer occurrence mostly comes from FLRs, far exceeding the upstream percentages in the H distribution (in this case a relevant percentage of FLRs is detected also in the D component). The higher resonance frequencies (f ≈ 66–86 mHz; Fig. 9d) detected during SOLMAX2 with respect to those detected during SOLMAX1 (f ≈ 58–74 mHz; Fig. 9c) are consistent with the results obtained by Vellante et al. (1996) who suggested that the resonant mode, in general, occurs at lower frequencies during higher solar activity conditions. The comparison

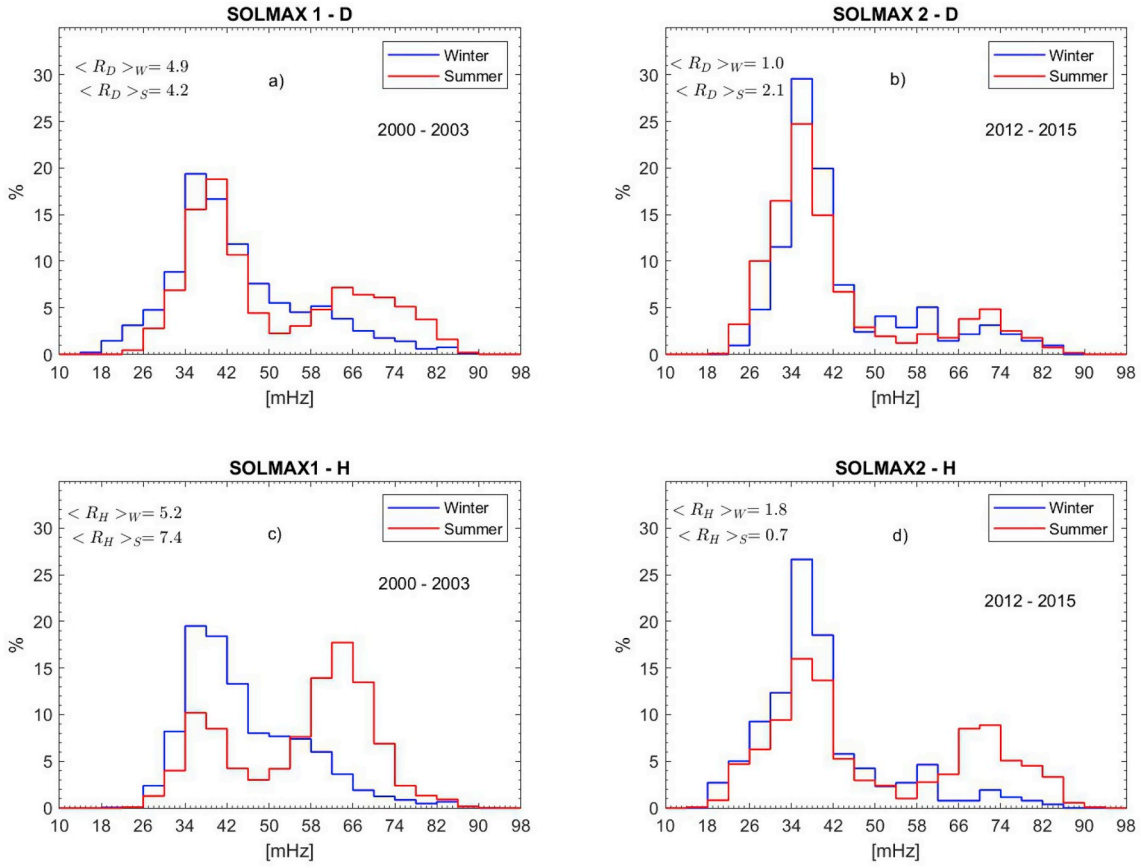

Fig. 9. a) The frequency distribution of the selected D events (winter, blue trace; summer, red trace) for SOLMAX1. b) The frequency distribution of the selected D events for SOLMAX2. c) The frequency distribution of the selected H events for SOLMAX1. d) The frequency distribution of the selected H events for SOLMAX2. (For interpretation of the references to colour in this figure legend, the reader is referred to the Web version of this article.)

between seasons confirms a tendency of lower resonance frequencies to occur during the winter (Fig. 9c).

7. Summary and discussion

Following previous analysis (Villante and Tiberi, 2015, 2016), we examined the solar cycle and seasonal modulation of the occurrence and characteristics of the relevant wave events in the mid-frequency ULF range ($f \approx$ 20–100 mHz) detected at a low latitude ground-based station (L'Aquila, Italy) between ≈1996–2015. For this scope, we examined ≈51,000 events on each component, H and D, with several interesting results.

a) For comparable SW speeds, during the winter the dayside wave activity appears more intense than during the summer; in addition, the winter activity mostly consists of upstream waves, with some predominance of D events (Figs. 4 and 5). This suggests a seasonal dependence of the attenuation and rotation of the downgoing signal through the ionosphere and, during winter, less efficient ionospheric conditions for the onset of relevant FLRs. These aspects might be related to the lower electron densities in the E layer during the winter; on the other hand, the higher variability of *fo*F2 observed in the winter months (Pietrella et al., 2012) might well contribute to the higher ULF activity in ground observations. The comparison with earliest investigations suggests controversial results: according to Saito (1964), indeed, at L ≈ 1.3, the wave activity, in general, might be somewhat more intense in summer than in winter; on the other hand, in agreement with the present results, it attained minimum values in the summer during solar minimum. Our results reveal also a tendency of lower resonance frequencies to occur during the winter: this aspect is consistent with the annual modulation of the plasmaspheric density (determining the resonance frequency) which attains maximum values in December and minimum values in July (Vellante et al., 2007).

b) Lanzerotti et al.(1981) and Howard and Menk (2005) considered the much higher morning activity consistent with a source region close to the subsolar magnetopause; indeed, when the IMF orientation is along the nominal spiral, most of the propagating upstream waves are expected to be blown back toward the morning side of the magnetosphere where the quasi-parallel bow shock structure would also provide favourable conditions for the local generation of upstream waves. Our results suggest that these aspects more clearly occur during the winter, when the FLR contribution is poor: in this season, indeed, the event occurrence peaks at ≈08–09 LT and at ≈12–13 LT, suggesting a relevant penetration of the upstream waves through the morning flank of the magnetopause, together with waves penetrating through the nose region. On the other hand, an additional source for the wave activity around noon during the winter might come from the variability of the electron density in the F2-layer: indeed, as shown by Pietrella et al. (2012), a midday maximum of the *fo*F2 variability emerges in winter while it is poorly distinguishable in summer. During the summer the concurring contribution of the upstream and the resonant waves would rather determine a broad (and smoother) enhancement of the occurrence rate in a wide sector between ≈09 and 12 LT.

c) Rapidly increasing after midnight, during the summer, R_T shows a peak at ≈03–04 LT (remarkably, in summer, this peak might exceed the dayside level) and a minimum at ≈05–06 LT; during the winter, a similar, less pronounced profile is delayed about ≈1 h. The entire pattern appears related to ionospheric features: indeed, in both

seasons, the LT occurrence of the average R_T minima appears coincident with the occurrence of the average *fo*F2 minima; moreover, as for *fo*F2, the further R_T increase is much sharper during the winter. As a matter of fact, additional contributions to the ULF activity in this LT sector might come from the excitation of localized waves by the moving terminator (Yagova et al., 1999): given its variable position during the year, it would, indeed, enhance the wave activity at earlier LTs in summer and at later LTs in winter. Interestingly, Pietrella et al. (2012) evidenced the presence of peaks of the *fo*F2 variability around sunrise and interpreted these aspects in terms of sudden increase of the electron density caused by the turning on of the ionizing solar radiation. They also reported peaks of the *fo*F2 variability around sunset only in few cases, during low solar activity and mostly in November: consistently, we observed enhancements of the wave occurrence near dusk only at solar minima, in winter. At the same time, it should be mentioned that the enhanced wave activity near dawn is also in agreement with previous studies (Saka et al., 1980, 1982, 1988; Saka and Alperovich, 1993; Tanaka et al., 2004, 2007) that ultimately related it to the E-layer ionization at sunrise, with a consequent increase of the Hall and Pedersen conductivities, that reach their greatest values right at E-layer altitudes (Davies, 1990). According to these studies, the increase of such conductivities in the dawn sector makes it possible the closure through the E layer of magnetosphere-ionosphere three-dimensional current systems whose oscillations alter the pattern of magnetic signals recorded at the ground (Green and Hamilton, 1978; Rostocker and Lam, 1978; Saka et al., 1980, 1982; Imajo et al., 2016). Around sunset, concurrently with the disappearance of the E layer, and so with a significant decrease of the Hall and Pedersen conductivities, the additional contribution to the wave activity should be strongly reduced; similar features have been, indeed, rarely reported in the scientific literature (Imajo et al., 2015). More in general, it might be also interesting to remind that statistical studies of travelling ionospheric disturbances showed that they occur often near dawn (with a maximum rate in winter and a minimum rate in summer) and rarely near dusk (Song et al., 2013); this suggests that also these phenomena can somehow play a significant role in triggering the enhanced wave activity characterizing the dawn.

d) The analysis conducted for different phases of the solar cycle reveals that, during solar minima, the winter rate of the event occurrence (even in absence of an explicit winter anomaly) persists higher than during the summer; by contrast, differently from the average behavior, during solar maxima the summer wave activity exceeds the winter one: this feature might be mostly related to the more frequent impact on the magnetosphere of energetic SW structures during solar maxima; in summer, given the favourable ionospheric conditions, they might determine a much more frequent manifestation of relevant resonance events. The higher daytime wave activity detected in summer during solar maxima might be related also to the ionospheric variability; indeed, Pietrella et al. (2012) found that, for low solar activity, the daytime *fo*F2 variability is, on average, enhanced in winter, while, for high solar activity, it is enhanced in summer. In the past, Verő (1981) and Verő and Menk (1986), comparing winter and summer observations at northern mid-latitudes during solar maximum years, suggested a "winter damping" in the ULF activity in association with a local *fo*F2 increase above $\approx 10^{11}$ MHz. Interestingly, in substantial agreement with the present conclusions, Verő et al. (1995) re-examined data from stations (including AQU) located below $L \approx 3$ and concluded that the smaller winter activity was mostly related to the smaller occurrence of fluctuations above $f \approx 50$ mHz (i. e. mostly in the range of FLRs).

Acknowledgements

This research activity is supported by Consorzio "Area di Ricerca in Astrogeofisica", Geomagnetic data from AQU observatory can be obtained by contacting the corresponding author (umberto.villante@aquila.infn.it).

Appendix A. Supplementary data

Supplementary data to this article can be found online at https://doi.org/10.1016/j.jastp.2019.05.005.

References

Burns, A.G., Wang, W., Qian, L., Solomon, S.C., Zhang, Y., Paxton, L.J., Yue, X., 2014. On the solar cycle variation of the winter anomaly. J. Geophys. Res. Space Physics 119, 4938–4949. https://doi.org/10.1002/2013JA019552.

Chen, C.H., Huba, J.D., Saito, A., Lin, C.H., Liu, J.Y., 2011. Theoretical study of the ionospheric Weddell Sea anomaly using Sami2. J. Geophys. Res. Space Physics 116, A04305. https://doi.org/10.1029/2010JA015573.

Chen, C.H., Saito, A., Lin, C.H., Liu, J.Y., 2012. Long-term variations of the nighttime electron density enhancement during the ionospheric midlatitude summer. J. Geophys. Res. Space Physics 117, A07313. https://doi.org/10.1029/2011JA017138.

Davies, K., 1990. Ionospheric Radio. IEE Electromagnetic Waves Series, vol. 31. Peter Peregrinus Ltd., London, UK, p. 580pp.

Ezquer, R.G., Lopez, J.L., Scida, L.A., Cabrera, M.A., Zolesi, B., Bianchi, C., Pezzopane, M., Zuccheretti, E., Mosert, M., 2014. Behaviour of ionospheric magnitudes of F2 region over Tucuman during a deep solar minimum and comparison with the IRI 2012 model predictions. J. Atmos. Sol. Terr. Phys. 107, 89–98. https://doi.org/10.1016/j.jastp.2013.11.010.

Green, C.A., Hamilton, R.A., 1978. Polarization characteristics and phase differences of Pi2 pulsations at conjugate stations. J. Atmos. Terr. Phys. 40, 1223–1228. https://doi.org/10.1016/0021-9169(78)90072-7.

Hargreaves, J.K., 1995. The Solar Terrestrial Environment: an Introduction to Geospace. Cambridge University Press, p. 420pp.

Heilig, B., Sutcliffe, P.R., Ndiitwani, D.C., Collier, A.B., 2013. Statistical study of geomagnetic field line resonances observed by CHAMP and on the ground. J. Geophys. Res. Space Physics 118, 1934–1947. https://doi.org/10.1002/jgra.50215.

Howard, T.A., Menk, F.W., 2005. Ground observations of high-latitude Pc3-4 ULF waves. J. Geophys. Res. Space Physics 110, A04205. https://doi.org/10.1029/2004JA010417.

Imajo, S., Yoshikawa, A., Uozumi, T., Ohtani, S., Nakamizo, A., Marshall, R., Shevtsov, B. M., Akulichev, V.A., Sukhbaatar, U., Liedloff, A., Yumoto, K., 2015. Pi2 pulsations observed around the dawn terminator. J Geophys Res Space Physics 120 (3), 2088–2098. https://doi.org/10.1002/2013JA019691.

Imajo, S., Yoshikawa, A., Uozumi, T., Ohtani, S., Nakamizo, A., Demberel, S., Shevtsov, B.M., 2016. Solar terminator effects on middle to low-latitude Pi2 pulsations. Earth Planets Space 68, 137. https://doi.org/10.1186/s40623-016-0514-1.

Keiling, A., Takahashi, K., 2011. Review of Pi2 models. Space Sci. Rev. 161, 63–148. https://doi.org/10.1007/s11214-011-9818-4.

Lanzerotti, L.J., Medford, L.V., Maclennan, C.G., Hasegawa, T., Acuna, M.H., Dolce, S.R., 1981. Polarization characteristics of hydromagnetic waves at low geomagnetic latitudes. J. Geophys. Res. 86 (A7), 5500–5506. https://doi.org/10.1029/JA086iA07p05500.

Menk, F.W., 2013. Magnetospheric ULF waves: a review. In: Liu, W., Fujimoto, M. (Eds.), The Dynamical Magnetosphere. IAGA Special book, Springer. dx.doi.org/10.1007/978-94-007-0501-2_13.

Olson, J.V., Fraser, B.J., 1994. Pc3 pulsations in the cusp. In: Solar Wind Sources of Magnetospheric Ultra-low-frequency Waves. Geophysical Monogr., vol. 81. AGU, Washington, D.C, pp. 325–334.

Perna, L., Pezzopane, M., 2016. foF2 vs solar indices for the Rome station: looking for the best general relation which is able to describe the anomalous minimum between cycles 23 and 24. J. Atmos. Sol. Terr. Phys. 148, 13–21. https://doi.org/10.1016/j.jastp.2016.08.003.

Perna, L., Pezzopane, M., Ezquer, R., Cabrera, M., Baskaradas, J.A., 2017. NmF2 trends at low and mid latitudes for the recent solar minima and comparison with IRI-2012 model. Adv. Space Res. 60, 363–374. https://doi.org/10.1016/j.asr.2016.09.025.

Pezzopane, M., 2004. Interpre: a Windows software for semiautomatic scaling of ionospheric parameters from ionograms. Comput. Geosci. 30, 125–130. https://doi.org/10.1016/j.cageo.2003.09.009.

Pietrella, M., Pezzopane, M., Scotto, C., 2012. Variability of foF2 over Rome and Gibilmanna during three solar cycles (1976-2000). J. Geophys. Res. Space Physics 117, A05316. https://doi.org/10.1029/2011JA017462.

Pilipenko, V., Fedorov, E., Heilig, B., Engebretson, M.J., 2008. Structure of ULF Pc3 waves at low latitudes. J. Geophys. Res. Space Physics 113, A11208. https://doi.org/10.1029/2008JA013243.

Ponomarenko, P.V., Fraser, B.J., Menk, F.W., Ables, S.T., Morris, R.J., 2002. Cusp-latitude Pc3 spectra: band-limited and power-law components. Ann. Geophys. 20, 1539–1551. https://doi.org/10.5194/angeo-20-1539-2002.

Ponomarenko, P.V., Waters, C.L., St-Maurice, J.-P., 2010. Upstream Pc3-4 waves: experimental evidence of propagation to the nightside plasmapause/plasmatrough. Geophys. Res. Lett. 37, L22102. https://doi.org/10.1029/2010GL045416.

Rishbeth, H., Garriot, O.K., 1969. Introduction to Ionospheric Physics. Academic Press, New York and London, p. 334pp.

Rishbeth, H., Muller-Wodarg, I.C.F., Zou, L., Fuller-Rowell, T.J., Millward, G.H., Moffett, R.J., Idenden, D.W., Aylward, A.D., 2000. Annual and semiannual variations in the ionospheric F2-layer: II. Physical discussion. Ann. Geophys. 18 (8), 945–956. https://doi.org/10.1007/s00585-000-0945-6.

Romano, V., Pau, S., Pezzopane, M., Zuccheretti, E., Zolesi, B., De Franceschi, G., Locatelli, S., 2008. The electronic Space Weather upper atmosphere (eSWua) project at INGV: advancements and state of the art. Ann. Geophys. 26, 345–351. https://doi.org/10.5194/angeo-26-345-2008.

Rostoker, G., Lam, H.L., 1978. A generation mechanism for Pc5 micropulsations in the morning sector. Planet. Space Sci. 26, 493–505. https://doi.org/10.1016/0032-0633(78)90070-3.

Saito, T., 1964. Mechanism of geomagnetic continuous pulsations and physical state of the exosphere. J. Geomagn. Geoelectr. 16 (2), 115–151. https://doi.org/10.5636/jgg.16.115.

Saka, O., Alperovich, L., 1993. Sunrise effect on dayside Pc pulsations at the dip equator. J. Geophys. Res. 98 (A8), 13779–13786. https://doi.org/10.1029/93JA00730.

Saka, O., Iijima, T.-J., Kitamura, T., 1980. Ionospheric control of low latitude geomagnetic micropulsations. J. Atmos. Sol. Terr. Phys. 42, 517–520.

Saka, O., Itonaga, M., Kitamura, T., 1982. Ionospheric control of low latitude geomagnetic micropulsations at sunrise. J. Atmos. Terr. Phys. 44, 703–712.

Saka, O., Kitamura, T.I., Shimoizumi, M., Araki, T., Oguti, T., Veliz, O., Ishitsuka, M., 1988. The effects of non-uniform ionosphere on equatorial Pc3 pulsations. J. Geomagn. Geoelectr. 40, 635–643.

Song, Q., Ding, F., Wan, W., Ning, B., Liu, L., Zhao, B., Li, Q., Zhang, R., 2013. Statistical study of large-scale traveling ionospheric disturbances generated by the solar terminator over China. J. Geophys. Res. Space Physics 118, 4583–4593. https://doi.org/10.1002/jgra.50423.

Takahashi, K., Liou, K., Yumoto, K., Kitamura, K., Nosé, M., Honary, F., 2005. Source of Pc4 pulsations observed on the nightside. J. Geophys. Res. Space Physics 110, A12207. https://doi.org/10.1029/2005JA011093.

Takahashi, K., Hartinger, M.D., Malaspina, D.M., Smith, C.W., Koga, K., Singer, H.J., Frühauff, D., Baishev, D.G., Moiseev, A.V., Yoshikawa, A., 2016. Propagation of ULF waves from the upstream region to the midnight sector of the inner magnetosphere. J. Geophys. Res. Space Physics 121, 8428–8447. https://doi.org/10.1002/2016JA022958.

Tanaka, Y.-M., Yumoto, K., Yoshikawa, A., Shinohara, M., Kawano, H., Kitamura, T.-I., 2004. Longitudinal structure of Pc 3 pulsations on the ground near the magnetic equator. J. Geophys. Res. Space Physics 109, A03201. https://doi.org/10.1029/2003JA009903.

Tanaka, Y.-M., Yumoto, K., Yoshikawa, A., Itonaga, M., Shinohara, M., Takasaki, S., Fraser, B.J., 2007. Horizontal amplitude and phase structure of low-latitude Pc 3 pulsations around the dawn terminator. J. Geophys. Res. Space Physics 112, 11308. https://doi.org/10.1029/2007JA012585.

Troitskaya, V.A., 1994. Discoveries of sources of Pc2–4 waves: a review of research in the former USSR. In: Engebretson, M.J., Takahashi, K., Scholer, M. (Eds.), Solar Wind Sources of Magnetospheric Ultralow Frequency Waves, Geophys. Monogr. Ser., vol. 81. AGU, Washington, D. C, pp. 45–54.

Troitskaya, V.A., Plyasova-Bakunina, T.A., Gul'yel'mi, A.V., 1971. Connection of Pc2-4 pulsations with interplanetary magnetic field. Dokl. Akad. Nauk SSSR 197, 1312.

Vellante, M., Villante, U., De Lauretis, M., Barchi, G., 1996. Solar cycle variation of the dominant frequencies of Pc3 geomagnetic pulsations at L = 1.6. Geophys. Res. Lett. 23 (12), 1505–1508.

Vellante, M., Förster, M., Villante, U., Zhang, T.L., Magnes, W., 2007. Solar activity dependence of geomagnetic field line resonance frequencies at low latitudes. J. Geophys. Res. 112, A02205. https://doi.org/10.1029/2006JA011909.

Verő, J., 1981. Changes of pulsations activity during two solar cycles. J. Atmos. Terr. Phys. 43, 919–926.

Verő, J., Menk, F.W., 1986. Damping of geomagnetic pulsations at high F2 layer electron concentrations. J. Atmos. Terr. Phys. 48, 231–243.

Verő, J., Best, I., Vellante, M., Lühr, H., De Lauretis, M., Holló, L., Märcz, F., Struesutik, J., 1995. Relations of field line resonances and upstream waves and the winter attenuation of pulsations. Ann. Geophys. 13, 689–697. https://doi.org/10.1007/s00585-995-0689-4.

Villante, U., 2007. Ultra low frequency waves in the magnetosphere. In: Kamide, Y., Chian, A. (Eds.), Handbook of the Solar-Terrestrial Environment. Springer, pp. 397–422.

Villante, U., Tiberi, P., 2015. A comprehensive analysis of the occurrence and characteristics of midperiod ULF waves at low latitude. J. Geophys. Res. Space Physics 120, 1784–1802. https://doi.org/10.1002/2014JA020558.

Villante, U., Tiberi, P., 2016. Occurrence and characteristics of nighttime ULF waves at low latitude: the results of a comprehensive analysis. J. Geophys. Res. Space Physics 121, 4300–4315. https://doi.org/10.1002/2015JA022137.

Yagova, N.V., Pilipenko, V., Fedorov, E., Vellante, M., Yumoto, K., 1999. Influence of ionospheric conductivity on mid-latitude Pc 3– 4 pulsations. Earth Planets Space 51, 129–138.

Yagova, N.V., Heilig, B., Pilipenko, V.A., Yoshikawa, A., Nosikova, N.S., Yumoto, K., Reda, J., 2017. Nighttime Pc3 pulsations: MM100 and MAGDAS observations. Earth Planets Space 69, 61. https://doi.org/10.1186/s40623-017-0647-x.

Yedidia, B.A., Vellante, M., Villante, U., Lazarus, A.J., 1991. A study of the relationship between micropulsations and solar wind properties. J. Geophys. Res. 96, 3465–3470.

Zuccheretti, E., Tutone, G., Sciacca, U., Bianchi, C., Arokiasamy, B.J., 2003. The new AIS-INGV digital ionosonde. Ann. Geophys. 46 (4), 647–659. https://doi.org/10.4401/ag-4377.